IV Experiment to Detect Double-Λ Hypernuclei (E885)

The overall goal of strangeness physics studies is to achieve an understanding of the strong, weak, and electromagnetic properties of hypernuclei and the underlying hyperon-nucleon and hyperon-hyperon interactions. Such studies represent an extension of conventional nucleon-nucleon scattering experiments as strangeness introduces new degrees of freedom. More specifically, measurements of the $\Lambda\Lambda$ residual binding energy in double-Λ hypernuclei, along with their corresponding production and decay branching ratios, can allow for more insight into the appropriate description of two baryon forces. Furthermore, studies of the decay modes of double-Λ hypernuclei can provide indirect evidence concerning the existence of the so-called H particle, a six-quark state predicted to be stable against strong decay due to the attractive nature of the color magnetic force [1]. Another interesting possibility within the realm of strangeness physics is the study of the formation probability of Ξ hypernuclei. Moreover, it may be the case that we can study double-Λ hypernuclei through the decay of Ξ hypernuclei. However at this point in time, the emulsion-based experiments searching for double-Λ hypernuclei have been unable to obtain more than a single kinematically complete event for any one hypernuclear species. In addition, the two events reported in the 1960's [2, 3] and the recent KEK event [4] appear to give inconsistent $\Lambda\Lambda$ binding energies. A high statistics counter experiment is clearly needed, and this was the basis for E885.

The experimental program of E885 concentrated on studying the production of double-Λ hypernuclei both through direct production and through the alternative approach suggested by M. May of BNL of producing the hypernuclei from a tagged Ξ^- particle stopping in the production target. The experiment concurrently studied production of the H particle through both of these production mechanisms. Each of these processes will be discussed in more detail in the next section.

The proposal to perform this experiment was presented to the Program Advisory Committee of the Brookhaven Alternating Gradient Synchrotron (AGS) in February 1992. The collaboration consists of scientists from Brookhaven National Laboratory,Carnegie Mellon University, Kyoto University, Kyoto Sangyo University, Rutgers University, TRIUMF, University of Freiburg, University of Manitoba, and the University of New Mexico. It was approved for 1500 hours of beam time. Morgan May (BNL) and Gregg Franklin (CMU) are the co-spokespersons. The experiment was designed to utilize the 2 GeV/c K^- beam line, K^+ spectrometer, and detectors developed for our completed H particle search experiments E813 and E836. E885 completed its data acquisition phase last year running from February through June 1996.

IV.A Experimental Program

Fig. IV.A.1 shows the detector configuration for E885. The spectrometer was instrumented to detect, identify, and momentum analyze the scattered K^+ mesons from the $p(K^-,K^+)\Xi^-$ reaction. The aerogel Cherenkov detectors FC and BC1 were used to veto pions while the Cherenkov detector FC0 was used to veto protons. Chapter III contains a detailed discussion of the technique for producing tagged Ξ^-'s and the results from our E813 experiment clearly establish that the apparatus is working as designed. The other major pieces of the apparatus include out-of-beam detector systems, necessary to detect the decay products of the produced hypernuclei. On the left and right of the target were located large efficiency/solid angle neutron detectors. Above and below the target were located the scintillating fiber (scifi) detectors used to provide both position and pulse height information from the charged decay products.

IV.A.1 Production of Double-Λ Hypernuclei with Stopped Ξ^- Hyperons

The apparatus developed for our H particle search experiments has proven successful in providing a tagged beam of Ξ^- hyperons. In E885, the same apparatus was used to tag events in which Ξ^-'s were stopped in our solid target. This solid target was formed from small cubes of synthetic diamond glued together to yield a target 8 cm (x) $\times$ 1 cm (y) $\times$ 5 cm (z). The density of the target was 3.3 gm/cm^3. A diamond target was chosen over CH_2 (ρ=0.94 gm/cm^3) or graphite (ρ=2.3 gm/cm^3) due to the fact that the higher density would result in more stopped Ξ^-'s within the target. The stopped Ξ^- hyperons and subsequent atomic capture by ^{12}C atoms, will allow us to determine the binding energy of $^{12}_{\Lambda\Lambda}$B through the reaction:

$$(\Xi^-,^{12}C)_{atom} \rightarrow^{12}_{\Lambda\Lambda} B + n.$$

Observation of the mono-energetic neutron in coincidence with a stopping Ξ^-, identifies the formation of $^{12}_{\Lambda\Lambda}$B, and the neutron energy is used to determine the $^{12}_{\Lambda\Lambda}$B mass. This hypernucleus consists of 5 neutrons, 5 protons, and 2 Λ particles. The $p_\Lambda s_\Lambda$ states with ^{10}B core in its ground state or at low excitation energy are expected to be most strongly populated. In this case the neutron energy is 12 MeV if we assume that the binding energy due to the attraction between the two Λ's is 4.5 MeV (consistent with the emulsion experiment results) and that p_Λ is 10 MeV above s_Λ. We have calculated that the $^{12}_{\Lambda\Lambda}$B mass can be measured to 0.5 MeV using this method.

The number of double-Λ hypernuclei created is directly dependent on the number of

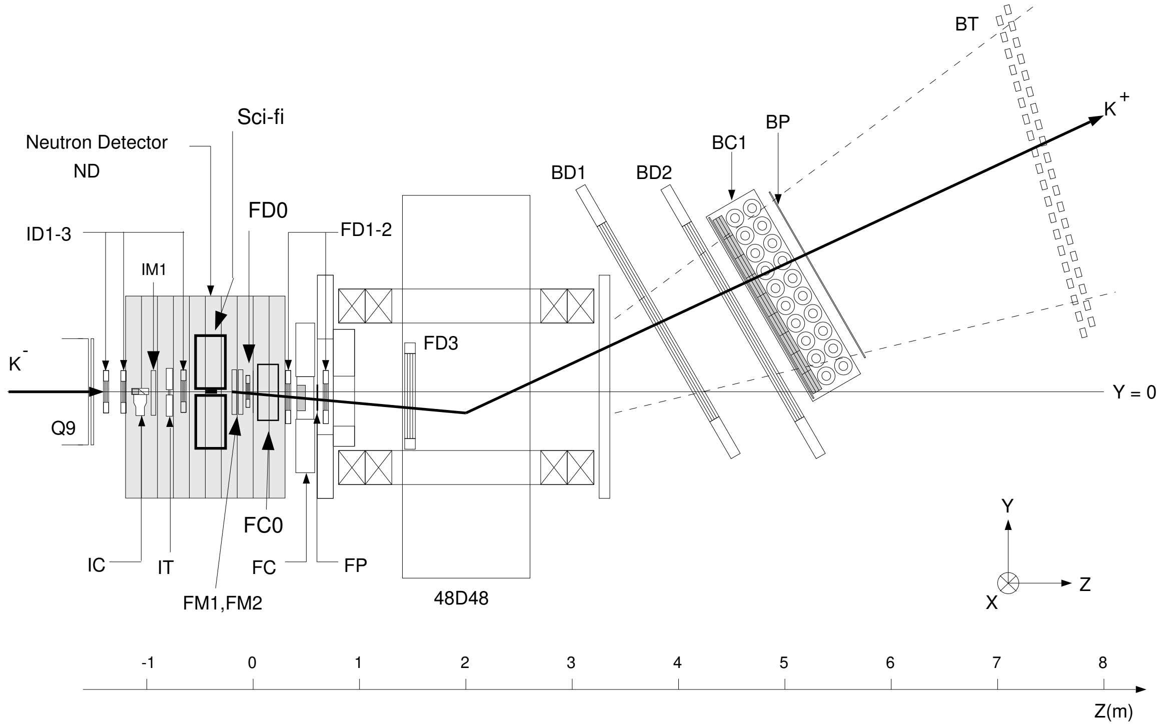

Figure IV.A.1: Detector configuration for E885. Drift chambers ID1, ID2, and ID3, along with the micro-strip chamber IM1 determine the incoming K $^{-}$ trajectory and are combined with upstream hodoscope data to determine the K^{-} momentum. Drift chambers FD0 through FD3, BD1, BD2, and micro-strips FM1 and FM2 determine the K^{+} trajectory through the spectrometer. Scintillators IT and BT determine the K^{+} time-of-flight. Hodoscopes FP and BP determine the spectrometer acceptance. Aerogel Cherenkovs IC, FC, and BC1 reject pions, while FC0 rejects protons. Above and below the target are the scintillating fiber detectors. On the left and right of the target are the large efficiency/solid angle neutron detectors.

cascades that were stopped within the target. The Monte Carlo calculations indicate that the Ξ^- stopping rate, defined as the ratio of stopped Ξ^-'s in the target to the number of tagged K^+'s in the spectrometer, to be nearly 6%. For the 1996 running sequence we had over 8×10^{11} K^-'s incident upon the diamond target, leading to an expected number of stopped Ξ^-'s in the target at about 20 000. This represents an increase of two order of magnitude in the number of stopped Ξ^-'s of all previously reported double-Λ hypernuclear searches combined.

Various theoretical calculations for the branching ratio of the $(\Xi^-,{}^{12}C)_{atom}$ decay into ${}^{12}_{\Lambda\Lambda}B$ + n fall in the range 5% to 20%. Beyond searching our neutron energy histograms for the signature mono-energetic peak, we also hope to be able to search for decay products from the ${}^{12}_{\Lambda\Lambda}B$ system in our scifi detectors to further identify and understand the reaction. These decay products include protons and pions from non-mesonic and mesonic decay, respectively, of the bound Λ's, as well as characteristic Σ^-p decays of the $\Lambda\Lambda$ pair.

IV.A.2 Direct Production of Double-Λ Hypernuclei

As described above, a diamond target was used to produce stopping Ξ^-'s. Double-Λ hypernuclei may also be produced directly by the reaction:

$$K^- +^{12} C \rightarrow^{12}_{\Lambda\Lambda} Be + K^+.$$

In this two-body reaction, missing mass gives the spectrum of hypernuclear states. A search can be made for double-Λ hypernuclei produced in this manner concurrently with the ${}^{12}_{\Lambda\Lambda}B$ experiment although the target is thicker than would be optimal for good resolution. The energy loss of the K^- and K^+ traversing the full thickness of the target is 40 MeV.

Because of the large momentum transfer, this reaction usually leads to continuum states. Calculations of the cross section for the reaction to individual bound states have been made for incident 1.1 GeV/c K^-'s, giving a prediction of 12 nb/sr [5]. Cross sections should be higher for 1.8 GeV/c K^-'s because 1.1 GeV/c is below threshold for Ξ^- production while 1.8 GeV/c is at the peak of the two-body Ξ^- production cross section. Additionally, up to an order of magnitude increase might result from small admixtures between the allowed double-strange hypernuclear states. Here, however, we assume the 1.1 GeV/c cross section which we regard as a lower limit.

Approximately 15 MeV is required to remove a Λ from the ${}^{12}_{\Lambda\Lambda}Be$ ground state. Thus even the modest resolution of the K^+ spectrometer should be sufficient to select out the $\Lambda\Lambda$ hypernuclear region. Also, 24 MeV is required for ${}^{12}_{\Lambda\Lambda}Be$ to fission into two Λ hypernuclei (somewhat more if the Coulomb barrier is taken into account). We therefore have a 24 MeV region in which detection of two sequential nucleon-stimulated weak decays (which can only occur within a hypernucleus) would signal a double-Λ hypernucleus. The apparent observation of one such sequential weak decay of two Λ's has recently been reported and discussed in the literature [4, 6].

The out-of-beam detector instrumentation will permit measurements of the lifetime and branching ratios of various decay modes. In a $\Lambda\Lambda$ hypernucleus, new weak decay modes are possible. We may observe the weak interaction between two Λ particles,

$$\Lambda\Lambda \rightarrow \Lambda n, \quad \Sigma^{-}p, \quad \Sigma^{0}n.$$

The branching ratio for each of these channels has been estimated to be in the 3-6% range [7]. The scifi detectors are able to detect the energetic Λ's ejected from the target with a characteristic decay length of 3 cm. This would result in a few detected $\Lambda\Lambda \rightarrow \Lambda$n events from $^{12}_{\Lambda\Lambda}$Be decays.

IV.A.3 H Particle Production

If the H particle exists we will be sensitive to it in two separate manners. First, Aerts and Dover [6] have indicated that the H particle could be produced in the direct reaction process:

$$K^{-} +^{12} C \rightarrow K^{+} + H + X.$$

This quasi-free production process will result in a peak in the (K^{-},K^{+}) missing mass spectrum. This approach, expected to be sensitive to more deeply bound H particles, has been applied in an experiment at KEK [8]. The spectra that we obtain in the course of this analysis should increase the sensitivity to H particles by several orders of magnitude due to our much larger statistical precision.

Another technique available to study the existence of the H particle involves production via stopped Ξ^{-}'s,

$$(\Xi^{-},^{12} C)_{atom} \rightarrow H +^{11} B.$$

The signature of the H particle formation would be provided through characteristic decays into Σ^{-}p within the scifi detector. Note that detection of the decay products of these various S=-2 systems is necessary to distinguish near-threshold H production from double-Λ hypernucleus production. This search is expected to be more sensitive to short-lived or more weakly bound H particles. Again, this process has been studied at KEK [8]. The main experimental goal of this search is not just to identify the formation of the H dibaryon, but also to be able to place accurate limits on its production probability, its mass, and its lifetime.

IV.A.4 Direct Production of Ξ^- Hypernuclei

For doubly strange systems, the possibility of examining the $\Lambda\Lambda$ force is the ultimate goal. A subsidiary but related goal is to answer the question: Is there a spectroscopy of Ξ hypernuclei? There are strong theoretical hints that such states exist because of the rather limited phase space available for their conversion into non-strange systems. In E885 we can search for evidence of these hypernuclei through the direct production process:

$$K^- +^{12} C \rightarrow^{12}_{\Xi} Be + K^+.$$

The signature would be a distinctive narrow peak, roughly 2 MeV in width, in the (K^-,K^+) missing mass spectrum. Although our system resolution is certainly not at this level, we may be able to study the major shell structure and the binding. From this information the Ξ^- single particle well depth can be determined and the strength of the $\Xi N \rightarrow \Lambda\Lambda$ interaction can be studied.

This reaction has been studied at KEK [8]. Reports on the Ξ^- hypernucleus production cross section give predictions in the range 100-336 nb/sr. This data will also provide information concerning the existence of $\Lambda\Lambda$ hypernuclei through the decay channel:

$$^{12}_{\Xi}Be \rightarrow^{11}_{\Lambda\Lambda} Be + n.$$

This decay path is expected to occur with a 20% branching ratio [9]. The mono-energetic neutron produced (expected to be 12 MeV) will provide a measure of the difference in binding energies of these hypernuclear species.

IV.B Performance of the Hardware

The protons from elastic and inelastic K^-p scattering dominated the trigger rate for E813 and E836, and it was expected that the rate of these reactions would be even larger in the double-Λ experiment due to the increased target mass and density. Although the FC0 Cherenkov was reasonably efficient at separating kaons and protons, even its small inefficiency could still potentially overwhelm the overall trigger rate. To further reduce the trigger rate from protons, a fast second level trigger relying on time of flight (TOF) was a necessity. However, since the momentum spectrum and path length of the scattering particles through the spectrometer was so diverse, a single TOF cut for all possible tracks was not sufficient.

Instead the tracks were classified in terms of FD3 wire cluster number (y-position in the 48D48 magnetic field aperture) and BT log number (y-position at the back hodoscope). This characterization was sufficient to break the acceptance into small regions so that only one cut was needed for each region. By knowing the position of the track at FD3 and its final position at BT, the particle's momentum was reasonably established so that a TOF cut could distinguish kaons from protons. A similar second level trigger was employed for E813, using hardware that required $\sim$150 μsec to complete the decision! However this time delay was completely unacceptable for E885 due to the requirements of the scifi detectors. The E885 second level trigger decision was designed to take only $\sim$15 μsec to complete while normal event readout took on the order of 5 msec. The second level trigger cut was shown to accept nearly 100% of the scattered K^+'s and reject over 96% of the protons that slipped through the FC0 Cherenkov detector untagged.

The signal to noise ratio can potentially be significantly improved by tagging events with coincident energetic protons in the scifi arrays. We note that in a hypernucleus, in addition to the usual free decay modes of the Λ,

$$\Lambda \to p\pi^- \qquad \Lambda \to n\pi^0,$$

new weak decay processes can occur,

$$\Lambda p \to np \qquad \Lambda n \to nn.$$

Detection of the fast proton from the non-mesonic decay clearly identifies the decay of a Λ which was bound to a nucleus. The Q-value of these non-mesonic decays is approximately 180 MeV so that the final state nucleon typically has 90 MeV kinetic energy as opposed to 5 MeV for the nucleon in free Λ decay. In hypernuclei with mass number A $\geq$ 10, the non-mesonic decays are 5 times more numerous that the decays accompanied by a pion.

The major new pieces of hardware incorporated into the detector system for E885 relative to our earlier H particle experiments were the addition of three X-Y reading micro-strip gas chambers (MSGC) and the two scintillating fiber detectors. The three MSGC detectors, designed and developed by the University of Manitoba and TRIUMF, each consisted of a single X-coordinate measuring plane and a single Y-coordinate measuring plane. One MSGC was placed upstream of the production target, and two MSGC's were placed downstream of the target. These chambers were employed to aide in the (K^-,K^+) track reconstructions. These detectors should allow for a better determination of the kaon path length through the dense diamond target for energy loss corrections, as well as allow for a better determination of the Ξ^- production vertex. The active area of each MSGC was roughly 8 cm (X) $\times$ 5 cm (Y). The lithographed substrate consisted of gold on a Upilex backing. The surface was sputtered with Ni/NiO to increase the surface resistivity to between 10^{11} and 10^{14} Ω to eliminate the need for a backplane potential. The anode strips were 40 μm wide and the cathode strips were 280 μm wide with an anode separation of 500 μm.

The chambers were plagued by high frequency noise pickup that could not be fully shielded. To combat the pickup, we were forced to increase their associated timing discriminator thresholds. This substantially reduced the overall micro-strip efficiency. Nevertheless, the hit information that was provided from these detectors will be incorporated into the tracking software reconstructions to improve our overall resolution.

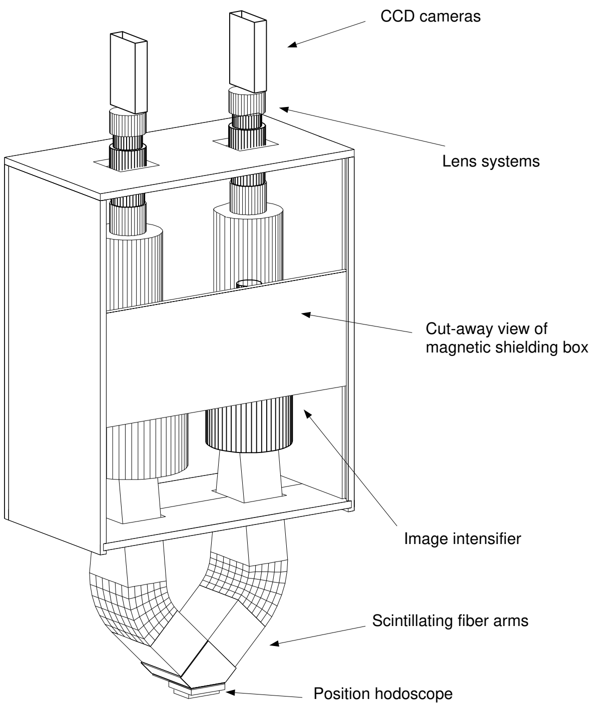

Figure IV.B.1: Schematic cut away view of one of the scintillating fiber detectors in its magnetic shielding box. Above the U-shaped scintillating fiber section are the two image intensifier units and the lens systems. Each leg of the detector is read out with a CCD camera.

During 1995 the two scintillating fiber detectors were designed and constructed at CMU. Each detector was constructed out of 1 mm $\times$ 1 mm scintillating fibers. Each fiber was clad in a thin layer of acrylic to provide internal reflection, and then covered with a thin layer of white paint to eliminate any fiber-to-fiber cross talk. Each fiber block consists of 7800 fibers arranged in a U-V readout as shown in Fig. IV.B.1. The fibers were arranged in boomerang-shaped sheets, one fiber thick and 78 fibers wide. These sheets were then stacked into a U-shaped aluminum box with alternating layers going up the two legs of the box.

Each leg of the scifi detectors was viewed by a multi-stage image intensifier (IIT) system. CMU currently owns two of these units, and the other two were borrowed from KEK. The IIT systems each consist of three different amplification stages. The last two stages contain micro-channel plates that could be gated such that their high voltage was not applied until the electronics second level trigger condition was satisfied. During this decision time the image was 'stored' on a phosphor screen within the unit. A lens system mounted to the end of each IIT focussed the image onto a DALSA CCD camera. The DALSA camera is a commercial unit with a digital output which can take pictures at a rate of up to 200 Hz, although due to limitations of the IIT systems, the rate was kept below 60 Hz. The DALSA camera digitizes the 256 $\times$ 256 pixel CCD array, and passes the 8-bits of amplitude information (65536 words) using standard TTL protocol.

As most of these data words were actually zero, CMU built electronics to zero suppress and compress this data as it was being transferred to the VME-based data acquisition system. This involved a small printed circuit board that mounted directly onto the camera to convert the TTL output into ECL, and then drove the signals to a front end processing printed circuit board. This ECL module compared each data word from the camera with an adjustable threshold, and suppressed all data under the threshold. The output from this module was the pixel address (row and column) and its data. The 65536 words sent from the camera were reduced to less than 500 words per picture from each camera.

Throughout most of the diamond target running, the pictures from the scifi detectors remained of satisfactory quality. However we found that the quality of the images was sensitive to several factors. Of primary importance was the beam tune. Care had to be taken to tune the beam to maximize the K^-/π^- ratio and the overall incident flux to limit the number of accidental tracks in the scifi images. A large accidental background in these images lead to pictures overflowing with tracks that would make extraction of the tracks of interest extremely difficult, if not impossible. The other factor which dictated the quality of the images was the sensitivity of the CCD cameras to the relative humidity in the experimental area. The higher the humidity level, the worse the pictures became. This sort of background manifested itself as a uniformly distributed low amplitude background of pixels beneath the charged particle tracks. Ultimately a compromise had to be reached between removing this background by increasing the front end board threshold and the loss of track information incurred by the higher thresholds.

IV.C Image scanning

About 40000 scifi images that passed the missing mass cut are currently being eye-scanned by 10 undergraduate students in Kyoto University. Figure IV.C.2 shows Ξ^- decay in two projections. The following event categories were defined:

- Event pattern of H$\rightarrow$ $\Sigma^- p$.
- V-track (decay of Ξ^-, Λ etc.)
- Stopping event in the fiducial of the scifi.
- Penetrating event from the fiducial.
- Multiple (>3) tracks from the same point.
- Other.

Each event will be scanned twice to reduce errors. The scanning is expected to be completed in June, 1998.

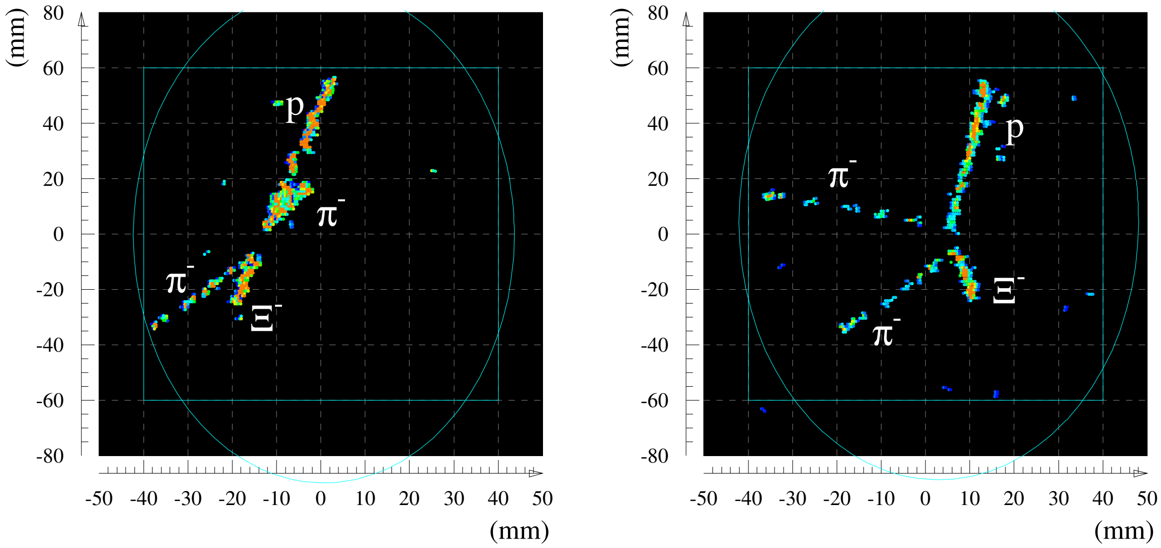

Figure IV.C.2: Scifi detector image showing the characteristic topology of Ξ^- decay: $\Xi^- \rightarrow \Lambda\pi^-, \Lambda \rightarrow p\pi^-$.